Interaction of mitochondrial targeting signals with acidic receptor domains along the protein import pathway: evidence for the 'acid chain' hypothesis

Tohru Komiya, Sabine Rospert[1], Carla Koehler[1], Renate Looser[1], Gottfried Schatz[1] and Katsuyoshi Mihara[2]

Department of Molecular Biology, Graduate School of Medical Science, Kyushu University, Fukuoka 812, Japan and [1]Biozentrum der Universität Basel, CH-4056 Basel, Switzerland

[2]Corresponding author
e-mail: mihara@cell.med.kyushu-u.ac.jp

Mitochondrial precursor proteins with basic targeting signals may be transported across the outer membrane by sequential binding to acidic receptor sites of increasing affinity. To test this 'acid chain' hypothesis, we assayed the interaction of mitochondrial precursors with three acidic receptor domains: the cytosolic domain of Tom20 and the intermembrane space domain of Tom22 and Tim23. The apparent affinity and salt resistance of precursor binding increased in the order Tom20<Tom22 (internal)<Tim23. Precursor binding to the three acidic receptor domains and to the pure cytosolic domain of Tom70 was inhibited by excess targeting peptide, but not by an equally basic control peptide. In this membrane-free and defined system, a precursor pre-bound to the Tom70 or Tom20 domain was transferred efficiently to the Tim23 domain. Transfer was stimulated by the internal Tom22 domain and was much less efficient in the reverse direction. Precursors destined for the outer membrane bound only to Tom20, but not to the internal Tom22 or the Tim23 domain, and a precursor destined for the inner membrane bound only to the Tom20 and the internal Tom22 domain, but not to the Tim23 domain. These results suggest that specific and sequential binding of a targeting signal to strategically situated acidic receptors delivers a precursor across the outer membrane and contributes to intramitochondrial sorting of imported proteins.
Keywords: import receptors/mitochondrial protein import/mitochondrial targeting signals/precursor proteins/precursor recognition

Introduction

Most precursor proteins destined to be imported from the cytoplasm into mitochondria are first bound to a cytosolic chaperone and then transferred from the chaperone to the protein import receptor on the mitochondrial surface. In the yeast *Saccharomyces cerevisiae*, this receptor consists of four distinct protein subunits that exist as two dynamically interacting subcomplexes: a heterodimer composed of Tom70 and Tom37, and a less well-characterized complex composed of Tom20 and Tom22 (Lill *et al.*, 1996; Schatz, 1996; Schatz and Dobberstein, 1996;

Neupert, 1997). The choice of receptor subcomplex appears to be determined by the cytosolic chaperone to which the precursor is bound. Cytosolic hsp70 delivers a bound precursor preferentially to the Tom20–Tom22 subcomplex in a reaction that does not require ATP hydrolysis. In contrast, the chaperone mitochondrial import-stimulating factor (MSF) delivers a bound precursor to the Tom70–Tom37 subcomplex in a reaction that requires ATP hydrolysis by MSF. The precursor is then transferred from Tom70–Tom37 to the Tom20–Tom22 subcomplex (Hachiya *et al.*, 1995; Komiya *et al.*, 1996; Mihara and Omura, 1996). These early steps of mitochondrial protein import have been reconstituted in a defined, membrane-free system with purified precursors, purified cytosolic chaperones and the recombinantly produced cytosolic domains of Tom70 and Tom20 (Komiya *et al.*, 1997).

Once bound to the import receptor, the precursor is transported across the protein-conducting channel (the TOM channel) in the outer membrane and its positively charged N-terminal targeting signal is then driven across the protein transport channel (the Tim23–Tim17 channel) in the inner membrane by the electric potential across that membrane. Finally, complete transport into the matrix is effected by the ATP-driven import motor, which is attached to the inner face of the inner membrane (Lill *et al.*, 1996; Schatz, 1996; Schatz and Dobberstein, 1996; Neupert, 1997).

Which force transports precursors across the outer membrane? The outer membrane, unlike the inner one, lacks an electric potential and an ATP-dependent protein transport motor. A possible answer was suggested by the findings that the cytosolic domains of Tom20 and Tom22 are highly acidic, that they bind the basic mitochondrial targeting signals and that this binding is salt-sensitive and thus presumably electrostatic (Lithgow *et al.*, 1994, 1995; Bolliger *et al.*, 1995; Haucke *et al.*, 1995; Hönlinger *et al.*, 1995; Mayer *et al.*, 1995b; Brix *et al.*, 1997; Komiya *et al.*, 1997; Schleiff *et al.*, 1997). Acidic domains capable of binding mitochondrial signal sequences are also present in Tom5, a small subunit of the TOM channel (Dietmeier *et al.*, 1997), and on the inner face of the outer membrane (Bolliger *et al.*, 1995; Mayer *et al.*, 1995a; Moczko *et al.*, 1997). Two of these internal binding sites have been identified as a small Tom22 domain exposed to the intermembrane space (Bolliger *et al.*, 1995; Moczko *et al.*, 1997) and a region on Tom40, a subunit of the TOM channel (Rapaport *et al.*, 1997). Still another potential binding site for mitochondrial signal sequences in the intermembrane space is a small acidic domain of Tim23, a subunit of the TIM channel (Bauer *et al.*, 1996). In principle, a precursor with a typical basic N-terminal targeting signal might thus be transported across the outer membrane by sequential binding to a relay of strategically

positioned acidic receptor sites of increasing affinity (Lithgow *et al.*, 1994; Bolliger *et al.*, 1995; Mayer *et al.*, 1995b; Dietmeier *et al.*, 1997; Schatz, 1997).

To test this 'acid chain' hypothesis (Hönlinger *et al.*, 1995; Schatz, 1997), we have assayed the interaction of mitochondrial precursors with three recombinantly produced acidic receptor domains: the cytosolic domain of Tom20, the intermembrane space domain of Tom22 and the intermembrane space domain of Tim23. We also included in these assays three additional proteins of the mitochondrial protein import system which are not strongly acidic: the cytosolic domain of the outer membrane receptor Tom70 and the purified cytosolic chaperones hsp70 and MSF. All receptor domains bound basic mitochondrial signal sequences; the apparent affinities increased in the order Tom70<Tom20<Tom22 (intermembrane space)<Tim23; transfer of a precursor from the Tom20 to the Tim23 domain was stimulated by the intermembrane space domain of Tom22; transfer of a precursor in the direction of the protein import pathway was much more efficient than in the reverse direction; and the Tim23 domain differed from the other domains in binding only precursors with a matrix-targeting signal, but not a precursor destined to be inserted into the inner membrane. The results obtained in this defined and membrane-free system thus seem to reflect specific and physiologically relevant interactions, which are compatible with the 'acid chain' hypothesis.

Results

The intermembrane space domain of Tom22 binds precursors that are transported completely across the mitochondrial outer membrane

The fusion protein MBP22 (Bolliger *et al.*, 1995) contains the 34 residue acidic intermembrane segment of Tom22 fused to the C-terminus of *Escherichia coli* maltose-binding protein (MBP). In order to test for interaction of this internal Tom22 segment with a matrix-targeted precursor protein, we bound purified [125I]pre-adrenodoxin (pAd) to purified cytosolic [125I]hsp70, incubated the resulting complex with either [125I]MBP22 or [125I]MBP, and subjected the mixtures to immunoprecipitation with IgGs against adrenodoxin. As shown in Figure 1A, pAd was completely transferred from hsp70 to MBP22 (lanes 1 and 2). No transfer was seen to MBP (lane 4): the hsp70–pAd complex was recovered intact in the immunoprecipitate (lane 3). Binding of pAd to MBP22 involved the precursor's N-terminal targeting signal as binding was completely inhibited by the synthetic mitochondrial targeting peptide SCC1-19 (lanes 5–8), but not by the equally basic, but non-functional control peptide SynB2 (lanes 9–12). Half-maximal inhibition by SCC1-19 was observed at ~2.0 μM (Figure 1B).

Similar results were obtained with three precursors which contain an uncleaved mitochondrial targeting signal and which are transported to the intermembrane space, the inner membrane and the matrix, respectively: *in vitro*-synthesized precursor of cytochrome *c* heme lyase (CCHL; Dumont *et al.*, 1987; Figure 1C); *in vitro*-synthesized ADP/ATP carrier (AAC; Pfanner *et al.*, 1987; not shown); and purified, urea-denatured cpn10 (Dubaquié *et al.*, 1997; not shown). In contrast, MBP22 did not bind *in vitro*-
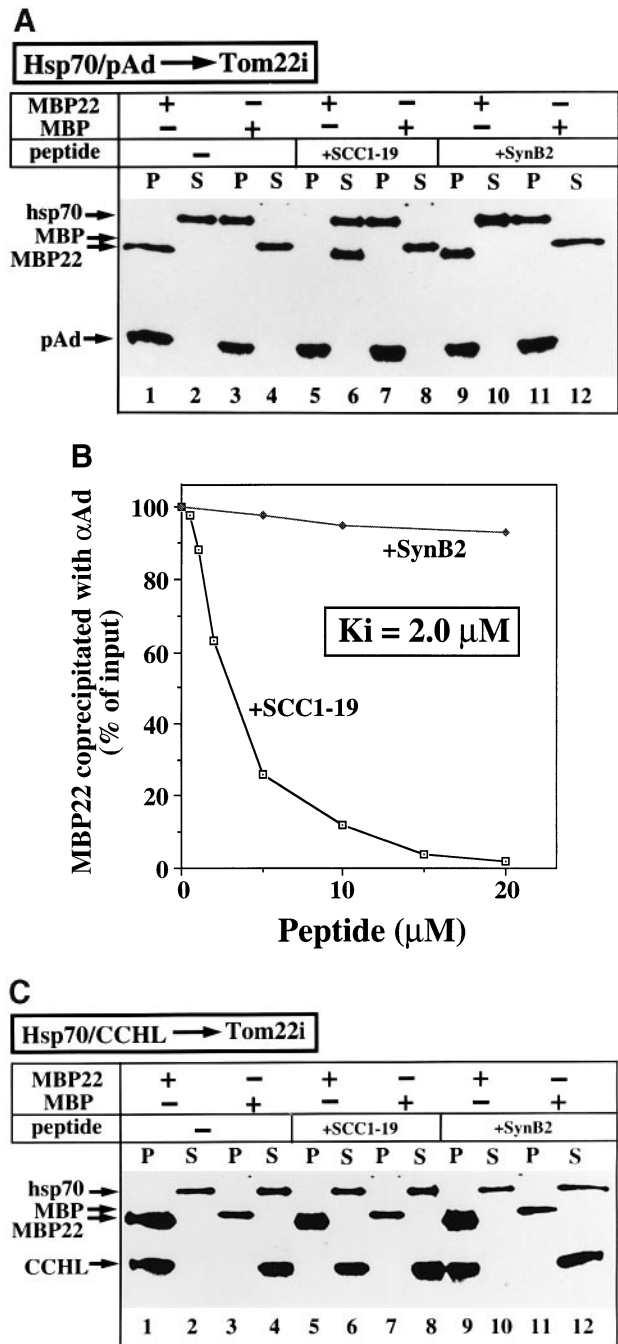

Fig. 1. Binding of pAd and CCHL to MBP22 is inhibited by a functional mitochondrial targeting peptide. (**A**) [125I]pAd pre-bound to [125I]hsp70 was incubated in 100 μl of T20K50M1 buffer at 30°C for 20 min with [125I]MBP22 or [125I]MBP in the presence or absence of 10 μM SCC1-19 (functional targeting peptide) or SynB2 (non-functional control peptide) and subjected to immunoprecipitation with 25 μg of IgGs against adrenodoxin (Ad). Immunoprecipitates (P) were washed twice with 20 mM phosphate buffer pH 7.0, 0.05% Tween-20, and the corresponding supernatants (S) were precipitated with 10% trichloroacetic acid (TCA). Both fractions were analyzed by SDS–PAGE and autoradiography. (**B**) Same as (A), but in the presence of the indicated concentrations of SCC1-19 or SynB2. The radioactivity of the immunoprecipitates was quantified. (**C**) [35S]methionine-labeled cytochrome *c* heme lyase (CCHL) was bound to [125I]hsp70 and then incubated with either [125I]MBP22 or [125I]MBP in the presence or absence of SCC1-19 or SynB2 as described above. Binding to [125I]MBP22 or [125I]MBP was assayed by immunoprecipitation with IgGs against MBP, SDS–PAGE and autoradiography. The efficiency of co-immunoprecipitation in the absence of added peptides (taken as 100% in the ordinate of the figure) was 95%.
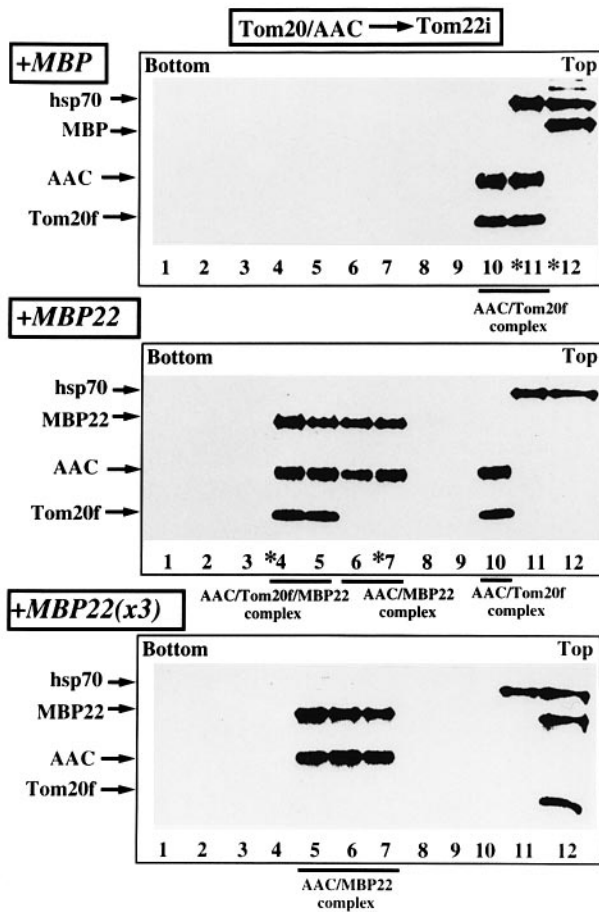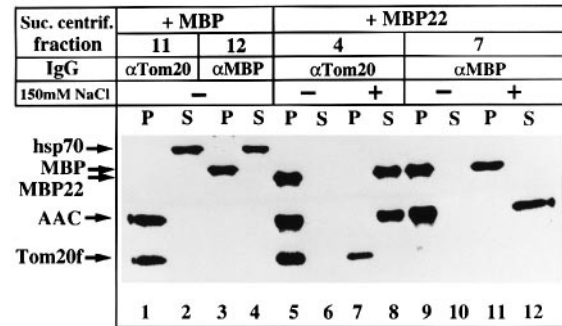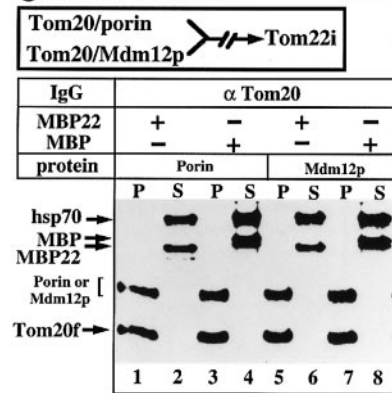
Fig. 2. AAC bound to Tom20f is transferred to MBP22 whereas Mdm12p or porin is not. (**A**) ^{35}S-labeled AAC was bound to [^{125}I]hsp70, then incubated in 500 μl of T20K50M1 buffer with [^{125}I]Tom20f, and finally with [^{125}I]MBP (+MBP), [^{125}I]MBP22 (+MBP22) or [^{125}I]MBP22 plus a 3-fold molar excess of unlabeled MBP22 [+MBP22 (×3)]. The reaction mixtures were subjected to sucrose density gradient centrifugation and fractions analyzed by SDS–PAGE and autoradiography. (**B**) The fractions indicated by numbers with asterisks in (A) were diluted 2-fold with distilled water and incubated with 25 μg of IgGs against Tom20 or MBP at 4°C overnight. Where indicated, NaCl was added to 150 mM and incubation continued for 5 min at 0°C. After addition of protein A–Sepharose and further incubation at 4°C for 2 h, proteins bound to the protein A–Sepharose were eluted with SDS-containing sample buffer. The eluted proteins (P) and the supernatants from the immunoprecipitation (S) were analyzed by SDS–PAGE and autoradiography. (**C**) [^{125}I]Porin or [^{35}S]methionine-labeled Mdm12p was subjected to the transfer reaction as described in (A). The reaction mixtures were subjected to immunoprecipitation with IgGs against Tom20 as described in Figure 1A.

synthesized Mdm12p or porin, two proteins which are inserted into, but not transported across, the outer membrane (Court *et al*., 1996b; Berger *et al*., 1997) (see Figure 2C below). These results confirm that MBP22 binds basic, N-terminal mitochondrial targeting signals (Bolliger *et al*., 1995; Moczko *et al*., 1997). They also show that binding is restricted to precursors which are imported across the outer membrane into the mitochondrial interior.

Transfer of mitochondrial precursors from Tom20f to MBP22

Can a mitochondrial precursor be transferred from the cytosolic Tom20 domain to the intermembrane space domain of Tom22? We bound [^{35}S]AAC (Figure 2A) to [^{125}I]hsp70, incubated the complex first with [^{125}I]Tom20f and then with either [^{125}I]MBP22 or [^{125}I]MBP, and finally analyzed each reaction mixture by gradient centrifugation (Figure 2A). In the presence of MBP, hsp70 and MBP remained on the top gradient and the AAC–Tom20f

complex was recovered in fractions 10 and 11 (Figure 2A, +MBP). The labeled AAC in fraction 11 was co-immunoprecipitated by IgGs against Tom20f and was thus present as a complex with Tom20f (Figure 2B, lanes 1 and 2). In the presence of MBP22, part of the AAC was transferred from Tom20f to MBP22 (Figure 2A, +MBP22, fractions 6 and 7; Figure 2B, lane 9) or to a MBP22–Tom20f complex (Figure 2A, +MBP22, fractions 4 and 5). In both cases, the co-migrating components were co-immunoprecipitated by anti-Tom20f IgGs or anti-MBP IgGs, confirming that they represented an AAC–MBP22 complex and an AAC–Tom20f–MBP22 complex (Figure 2B). Adding a 3-fold molar excess of unlabeled MBP22 to the reaction [MBP22 (×3)] shifted the equilibrium toward the AAC–MBP22 complex. The ternary AAC–Tom20f–MBP22 complex may thus be an intermediate in the transfer reaction.

Figure 2B also shows that both the AAC–MBP22 complex and the AAC–Tom20f–MBP22 complex are dissociated by 150 mM NaCl.
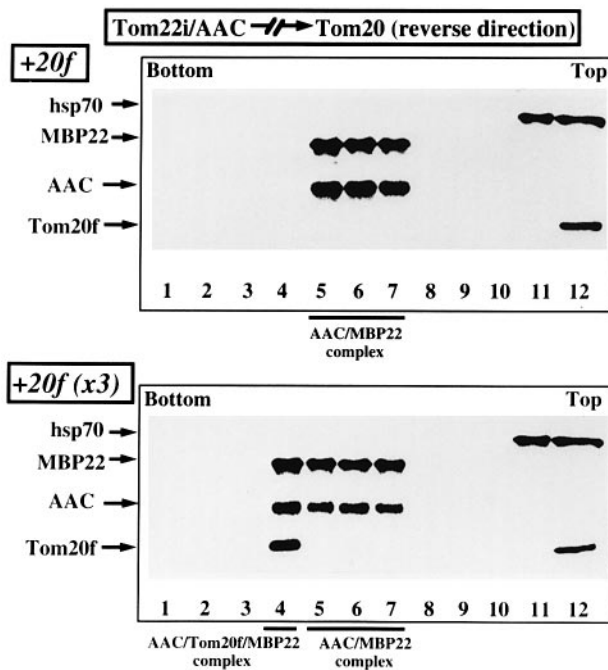
Fig. 3. AAC bound to MBP22 is not transferred to Tom20f. [^{35}S]methionine-labeled AAC was pre-bound to [^{125}I]hsp70 at 30°C for 20 min in 500 μl of T20K50M1 buffer. The resulting complex was incubated with [^{125}I]MBP22 at 30°C for 20 min and then with either [^{125}I]Tom20f (+20f) or with [^{125}I]Tom20f plus a 3-fold molar excess of unlabeled Tom20f [+20f (×3)]. Finally, the reaction mixtures were subjected to sucrose density gradient centrifugation as described in Figure 2A.

Analogous results were obtained for the matrix-targeted precursor [^{125}I]pAd (data not shown). However, the outer membrane proteins porin and Mdm12p behaved differently. In the experiment shown in Figure 2C, purified [^{125}I]porin or *in vitro*-synthesized [^{35}S]Mdm12p was bound to [^{125}I]hsp70; each complex was incubated with [^{125}I]Tom20f and then with either [^{125}I]MBP22 or [^{125}I]MBP; finally each mixture was analyzed by immunoprecipitation with anti-Tom20f gGs. Both precursors were transferred quantitatively from hsp70 to Tom20f, but there was no transfer to MBP22 (lanes 1, 2, 5 and 6). Thus, the intermembrane space domain of Tom22 fails to recognize precursors that do not traverse the outer membrane.

Precursor transfer from Tom20f to MBP22 is more efficient than the reverse reaction

Can AAC that is bound to MBP22 be transferred 'back' to Tom20f? [^{35}S]AAC was first bound to [^{125}I]hsp70 and then incubated with [^{125}I]MBP22 to allow formation of the AAC–MBP22 complex. When this complex was challenged with [^{125}I]Tom20f, subsequent gradient centrifugation showed that AAC remained quantitatively associated with MBP22 (Figure 3, +20f). This result was in striking contrast to that seen when the AAC–Tom20f complex was challenged with MBP22 (Figure 2A, +MBP22), even though the final concentrations of all components in the two experiments were identical. Even a 3-fold molar excess of unlabeled Tom20f to the AAC–MBP22 complex failed to cause significant transfer of AAC to Tom20f, although it did cause some formation of a ternary AAC–Tom20f–MBP22 complex [Figure 3, +20f
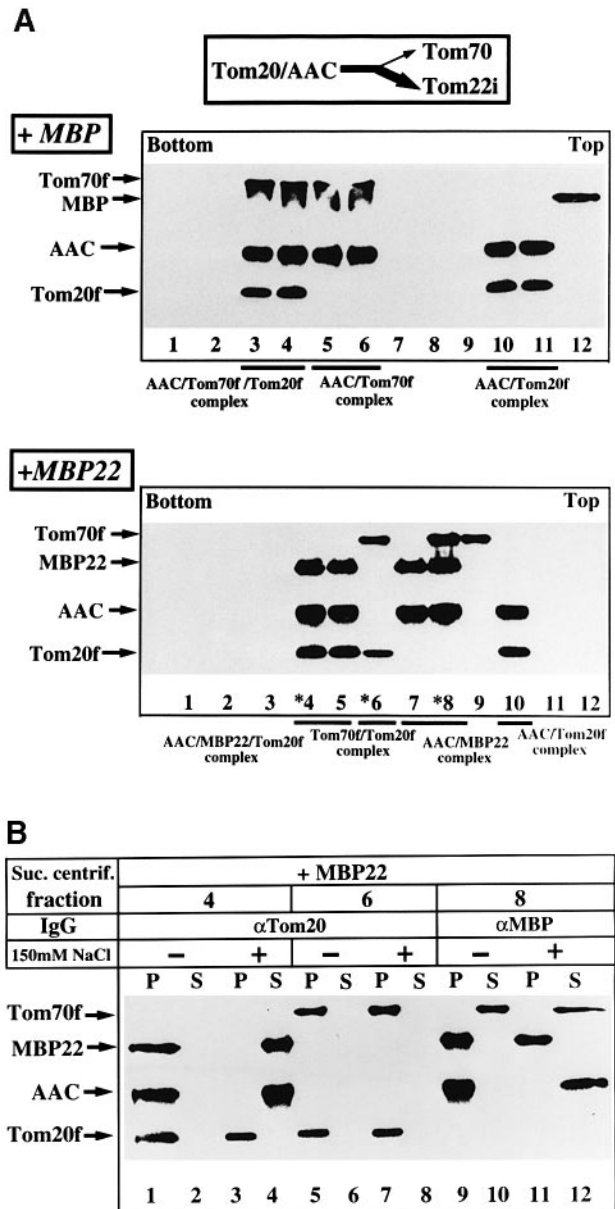

Fig. 4. Transfer of AAC from Tom20f to Tom70f is inhibited by the presence of MBP22. (**A**) ^{35}S-labeled AAC pre-bound to unlabeled hsp70 was incubated in 500 μl of T20K50M1 buffer with [^{125}I]Tom20f at 30°C for 20 min and then incubated with [^{125}I]Tom70f in the presence of either [^{125}I]MBP (+MBP) or [^{125}I]MBP22 (+MBP22) at 30°C for 20 min. The reaction mixtures were subjected to sucrose density gradient centrifugation as described in Figure 2A. Although not visible in this figure, repeats of the (+MBP22) experiment sometimes revealed a small amount of AAC in fraction 6. (**B**) The fractions indicated by numbers with asterisks in (A) were subjected to immunoprecipitation with IgGs against Tom20 or MBP and treated or not treated with 150 mM NaCl as in Figure 2B.

(×3), compare fractions 4 and 12]. In the system used here, the 'forward' reaction (transfer of AAC from Tom20f to MBP22) thus occurs much more readily than the reverse reaction.

Although pAd can be transferred from Tom20f to Tom70f *in vitro* (Komiya *et al.*, 1997), net transfer *in vivo* occurs from Tom20f to the intermembrane space domain of Tom22. If the system used here reflects the physiological situation, then MBP22 should compete effectively with

Tom70f for Tom20f-bound AAC. This was indeed the case. In the experiment shown in Figure 4, we pre-bound [^{35}S]AAC to unlabeled hsp70, then incubated the complex with [^{125}I]Tom20f to form the AAC–Tom20f complex, further incubated the mixture with [^{125}I]Tom70f in the absence (+MBP) or presence (+MBP22) of [^{125}I]MBP22, and finally analyzed both mixtures by gradient centrifugation (Figure 4A). In the absence of MBP22, AAC was partly transferred from the AAC–Tom20f complex (fractions 10 and 11) to the AAC–Tom70f complex (fractions 5 and 6) and the AAC–Tom70f–Tom20f complex (fractions 3 and 4), confirming our earlier report (Komiya *et al.*, 1997). MBP22 completely prevented formation of the AAC–Tom70f complex; instead the AAC–MBP22 complex (fractions 7 and 8) and the AAC–MBP22–Tom20f intermediate complex (fractions 4 and 5) accumulated, and the AAC–Tom20f complex decreased correspondingly. The existence of complexes in the fractions marked by an asterisk was verified by immunoprecipitation with IgGs against Tom20 or MBP (Figure 4B; see also Figure 9 in Komiya *et al.*, 1997).

The physiological 'forward' transfer of AAC from Tom20f to MBP22 is thus favored over the reverse reactions from MBP22 to Tom20f or from Tom20f to Tom70f. The same results were obtained for pAd (data not shown).

The acidic intermembrane space-exposed domain of Tim23 specifically binds matrix-targeted precursors

Tim23 is an essential component of the protein import system (the TIM system) in the mitochondrial inner membrane. Together with Tim17, it probably forms a protein-conducting pore across the inner membrane. However, Tim23 also contains an acidic N-terminal domain which protrudes into the intermembrane space and which has been suggested to function as a receptor for basic N-terminal mitochondrial targeting signals (Bauer *et al.*, 1996). In order to test whether this domain could be a link in the proposed 'acid chain' for basic mitochondrial targeting signals, we fused the domain to the C-terminus of bacterial glutathione-*S*-transferase (GST) and assayed the resulting water-soluble fusion protein GST23 for its interaction with mitochondrial precursor proteins.

In the first experiment, we pre-bound [^{125}I]pAd to unlabeled hsp70, challenged the complex with either [^{125}I]GST or [^{125}I]GST23, and assayed the mixture by immunoprecipitation with IgGs against adrenodoxin. GST23 efficiently bound pAd, but GST did not (Figure 5A, lanes 1–4). Binding required the precursor's targeting signal, as it was completely inhibited by the mitochondrial targeting peptide SCC1-19, but not by the equally basic control peptide SynB2 (lanes 5, 6, 9 and 10). Half-maximal inhibition occurred at ~0.6 μM SCC1-19 (Figure 5B). A similar result was obtained with cpn10, a matrix-targeted protein with an uncleaved N-terminal basic targeting signal (not shown). On the other hand, no binding was observed with AAC precursor which inserts into the inner membrane without traversing it completely (Figure 5C). This result agrees with the report that Tim23 only functions as the receptor for matrix-targeting signals, but not for the internal signal(s) of AAC and other multispanning carriers of the inner membrane (Sirrenberg *et al.*, 1996).
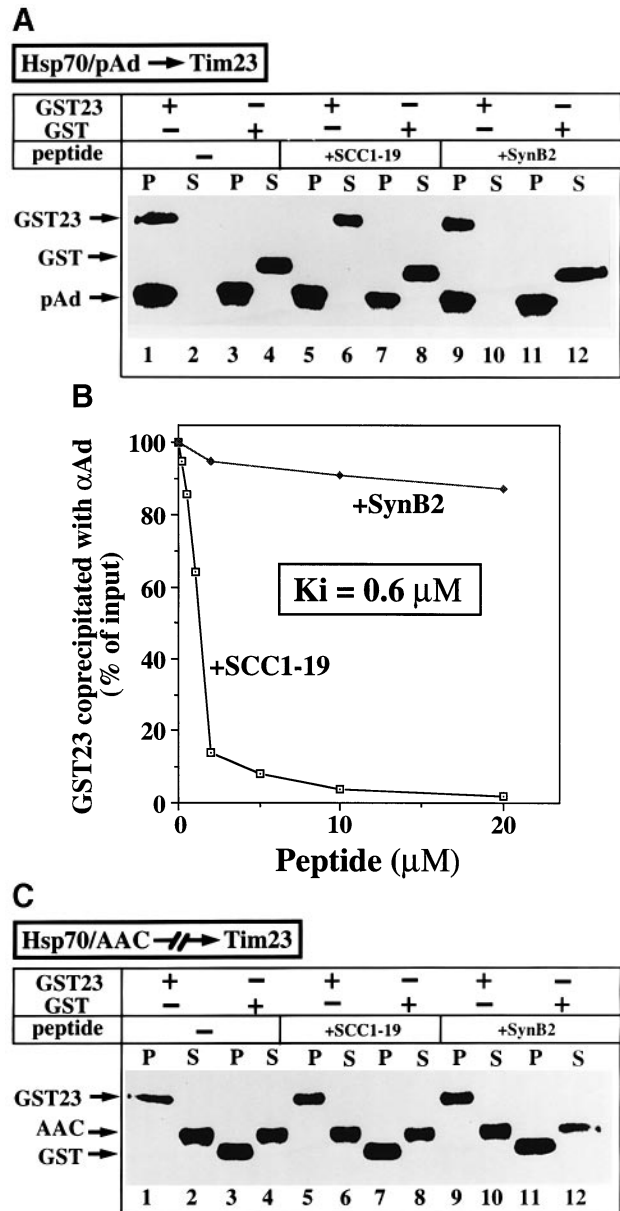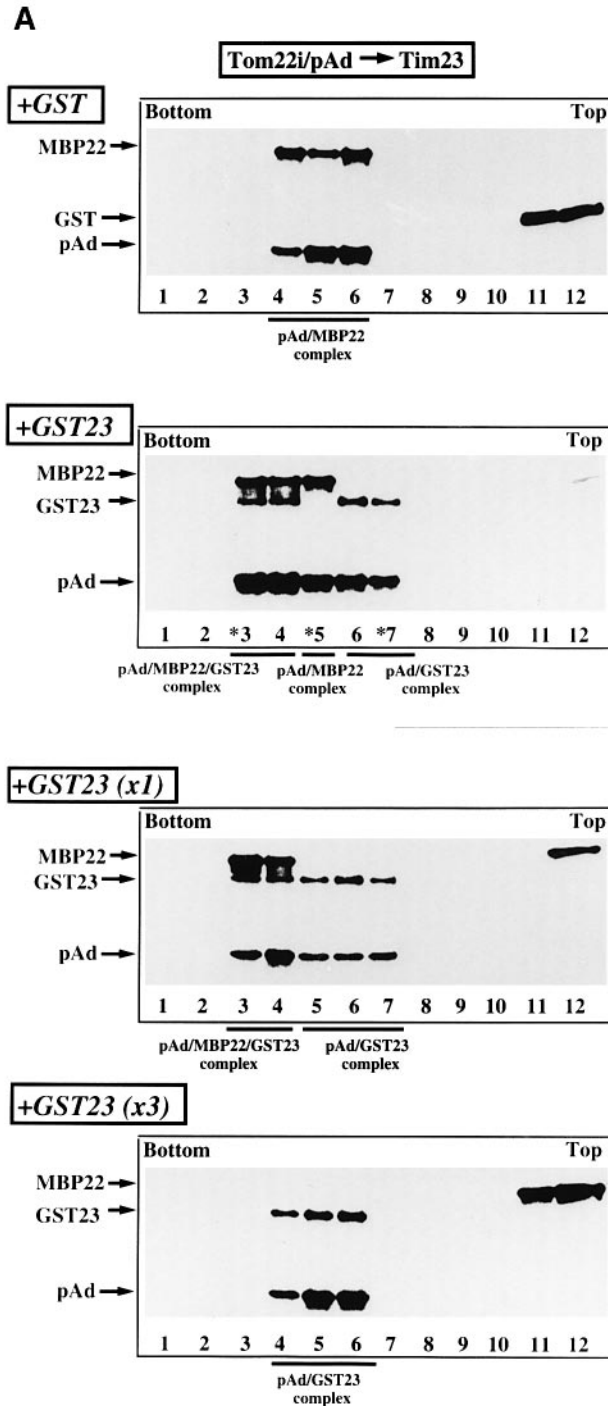

Fig. 5. pAd, but not AAC, binds to GST23 and binding is inhibited by a functional mitochondrial targeting peptide. (**A**) [^{125}I]pAd pre-bound to unlabeled hsp70 was incubated in 100 μl of T20K50M1 buffer with either [^{125}I]GST23 or [^{125}I]GST at 30°C for 20 min in the presence or absence of 10 μM SCC1-19 or SynB2. The reaction mixtures were subjected to immunoprecipitation with IgGs against adrenodoxin. Other conditions were as in Figure 1A. (**B**) The same experiments as in (A) but performed in the presence of the indicated concentrations of SCC1-19 or SynB2. (**C**) ^{35}S-labeled AAC pre-bound to unlabeled hsp70 was incubated in 500 μl of T20K50M1 buffer with [^{125}I]GST23 or [^{125}I]GST at 30°C for 20 min in the presence or absence of 10 μM SCC1-19 or SynB2. The reaction mixtures were incubated with glutathione–Sepharose. After centrifugation, supernatants (S) were precipitated with 10% TCA whereas the precipitates (P) were washed twice with 20 mM phosphate buffer pH 7.0, 0.05% Tween-20. Both fractions were analyzed by SDS–PAGE and autoradiography. The efficiency of co-immunoprecipitation in the absence of added peptides (taken as 100% in the ordinate of the figure) was 96%.

Transfer of a matrix-targeted precursor from MBP22 to GST23 is more efficient than the reverse reaction

During import into mitochondria, a matrix-targeted precursor would be expected to interact first with the internal

A

Tom22i/pAd → Tim23

+GST

+GST23

+GST23 (x1)

+GST23 (x3)

B

C

Tim23/pAd ⫫→ Tom22i

+MBP22

+MBP22(x3)

Fig. 6. pAd bound to MBP22 is transferred to GST23, but the reverse reaction is not observed. (A) [125I]pAd pre-bound to unlabeled hsp70 was incubated in 100 μl of T20K50M1 buffer with [125I]MBP22 at 30°C for 20 min to form the pAd–MBP22 complex. The complex was then incubated at 30°C for 20 min in the same buffer with [125I]GST, or with [125I]GST23 or [125I]GST23 plus either a 1- [+GST23 (×1)] or a 3-fold [+GST23 (×3)] molar excess of unlabeled GST23. Finally, each mixture was analyzed by gradient centrifugation. Other conditions were as described in Figure 2A. (B) The fractions indicated by numbers with asterisks in the '+GST23' experiment in (A) were subjected to immunoprecipitation with IgGs against adrenodoxin and then incubated in the absence or presence of 150 mM NaCl. Other conditions were as described in Figure 2B. (C) [125I]pAd pre-bound to unlabeled hsp70 was incubated sequentially in 100 μl of T20K50M1 buffer at 30°C for 20 min each with [125I]GST23 and with either [125I]MBP22 (+MBP22) or [125I]MBP22 plus a 3-molar excess of unlabeled MBP22 [+MBP22 (×3)]. The reaction mixtures were analyzed by gradient centrifugation and SDS–PAGE as in Figure 2A.

Tom22 domain and then with the exposed Tim23 domain. If the Tim23 domain bound the precursor more tightly than the internal Tom22 domain, unidirectional net transfer would ensue. To investigate this possibility, we bound [125I]pAd to unlabeled hsp70, added [125I]MBP22 to form the pAd–MBP22 complex, challenged this complex with either GST or GST23, and analyzed each mixture by gradient centrifugation. In the absence of GST23, only the pAd–MBP22 complex was detected (Figure 6A,
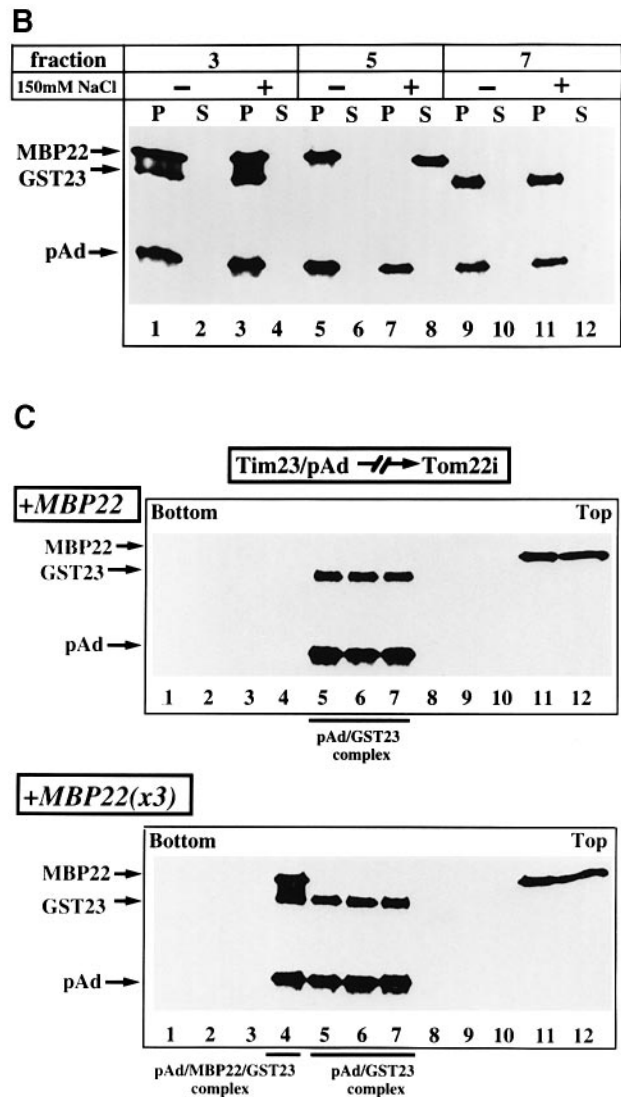
+GST). In the presence of GST23, this complex diminished and the pAd–GST23 complex as well as a pAd–MBP22–GST23 complex accumulated (Figure 6A, +GST23). The existence of the pAd–MBP22–GST23, pAd–MBP22 and pAd–GST23 complexes in gradient fractions 3, 5 and 7, respectively (Figure 6A, +GST23), was again confirmed by co-immunoprecipitation with IgGs against Ad (Figure 6B). The pAd–MBP22 complex dissociated at 150 mM NaCl (Figure 6B, lanes 7 and 8),
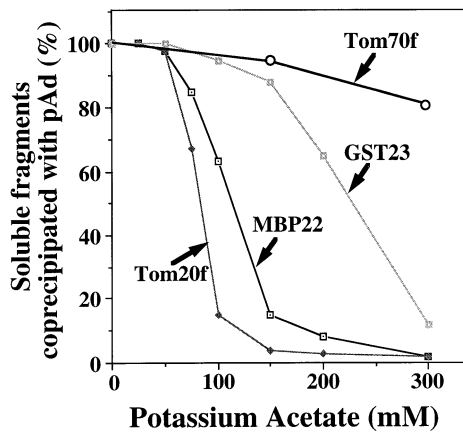
Fig. 7. Salt inhibits binding of pAd to Tom20f, MBP22 or GST23 to different degrees but does not inhibit binding to Tom70f. [^{125}I]pAd was pre-bound to [^{125}I]Tom70f, [^{125}I]Tom20f, [^{125}I]MBP22 or [^{125}I]GST23 in 100 μl of T20K50M1 buffer and then incubated sequentially with 25 μg of IgGs against Ad at 4°C overnight and with protein A–Sepharose at 4°C for 2 h. Immunoprecipitates were washed twice with 20 mM phosphate buffer pH 7.0, 0.05% Tween-20 and then incubated at 0°C for 5–10 min with 20 mM Tris–HCl buffer pH 7.5 containing the indicated concentrations of potassium acetate. The reaction mixtures were centrifuged, proteins were eluted from the protein A–Sepharose by SDS-containing sample buffer, and eluted proteins as well as proteins from the supernatant of the immuno-precipitation were analyzed by SDS–PAGE and autoradiography. The radioactivity of immunoprecipitates and supernatants was quantified. The efficiencies of co-immunoprecipitation in the absence of added potassium acetate (taken as 100% in the ordinate of the figure) for Tom70f, GST23, MBP22 and Tom20f were 95, 96, 95 and 94%, respectively.

whereas the pAd–GST23 and the pAd–MBP22–GST23 complexes were resistant to this salt concentration (Figure 6B, lanes 3, 4, 11 and 12; see also Figure 7). When a 1- or 3-fold molar excess of unlabeled GST23 over [^{125}I]GST23 was added, the amounts of the pAd–MBP22 and pAd–MBP22–GST23 complexes progress-ively decreased. In the presence of a 3-fold molar excess of unlabeled GST23, all of pAd accumulated as the pAd–GST23 complex, and all of the [^{125}I]MBP22 was released into the top fractions of the gradient.

An analogous test for 'reverse' transfer of pAd from GST23 to MBP22 failed to detect such a transfer: the entire pAd remained bound to GST23, and all of the added MBP22 was again recovered in the top fractions (Figure 6C). Even a 3-fold molar excess of unlabeled MBP22 did not induce formation of a pAd–MBP22 complex, although it did cause some of the pAd to accumulate in the putative transfer intermediate (the pAd–MBP22–GST23 complex) [Figure 6C, +MBP22 (×3)].

We conclude that pAd is transferred efficiently from the internal Tom22 domain to the extramembrane domain of Tim23, but is transferred only inefficiently in the opposite direction.

The pAd–Tom20f, pAd–MBP22 and pAd–GST23 complexes exhibit distinct salt sensitivity

The results reported here and earlier (Haucke *et al.*, 1995; Komiya *et al.*, 1997) have shown that binding of precursors to Tom20f is sensitive to 150 mM NaCl, whereas that to Tom70f is resistant to this salt concentration. Figure 7 compares the salt sensitivity of the different precursor–receptor complexes analyzed here. The pAd–Tom20f,

Table I. Summary of the apparent affinities of the import receptors for pAd and the half-maximum inhibitions by SCC1-19

Import receptors	K_d (nM)	K_i (μM)
Tom 70f	ND	5.0
Tom 20f	2.8	2.5
MBP22	1.6	2.0
GST23	0.54	0.6

ND, not determined.

pAd–MBP22 and pAd–GST23 complexes were all sensit-ive to potassium acetate, but to different degrees: half-maximal dissociation was observed at 90, 120 and 230 mM potassium acetate, respectively. The pAd–Tom70f complex was largely resistant even to 300 mM potassium acetate, confirming our earlier report. Salt resistance of precursor binding to the three acidic receptor domains thus increases in the same order as the apparent affinities. Similar results were obtained for AAC, except that it did not bind to GST23. Half-maximal dissociation of AAC from Tom20f or from MBP22 occurred at 105 and 135 mM potassium acetate, respectively (data not shown).

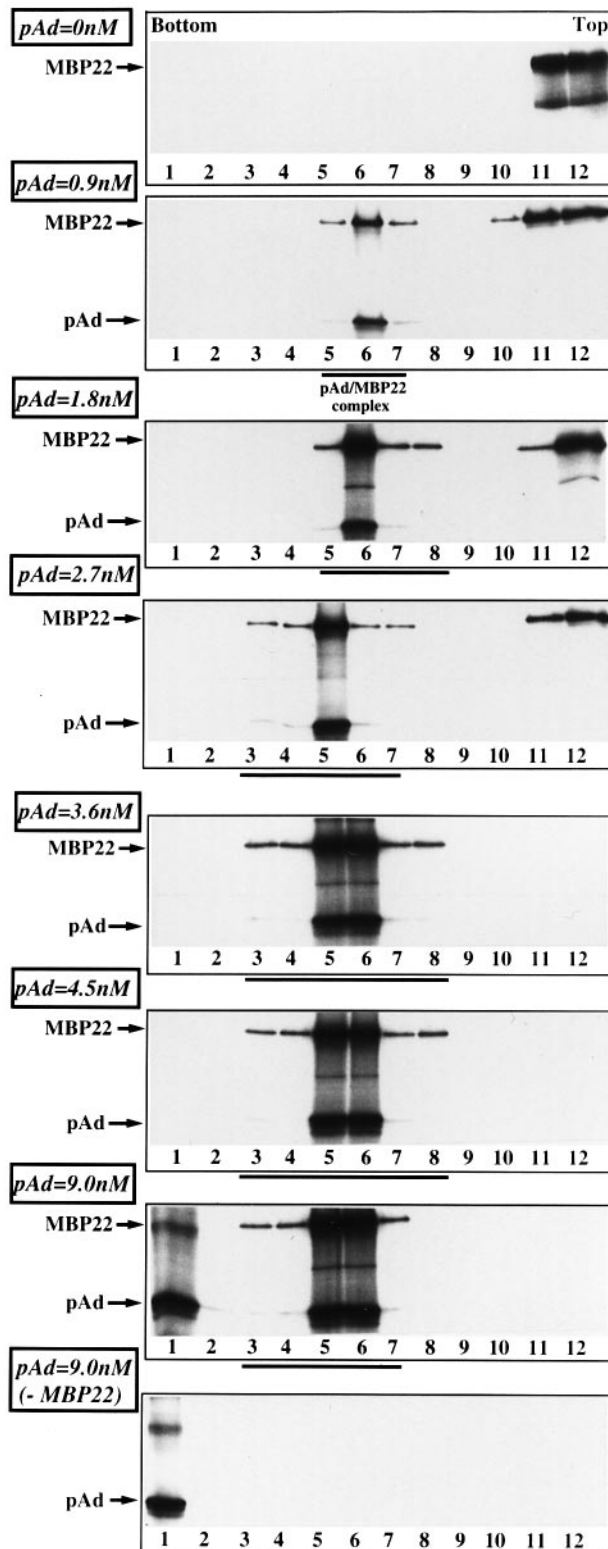### Determination of apparent affinities of Tom20f and the intermembrane space domains of Tom22 and Tim23 for pAd

The results described above suggest that the apparent affinities of the receptor domains for pAd increase in the order Tom20f<Tom22 (intermembrane)<Tim23 (inter-membrane). To test this prediction, we incubated a fixed amount of each receptor domain with different concentra-tions of pAd and measured formation of the receptor–pAd complex by sucrose density gradient centrifugation. The results with MBP22 are shown in Figure 8A. At low pAd concentration, both free MBP22 as well as the MBP22–pAd complex were detected, whereas higher pAd concen-trations yielded the MBP22–pAd complex and pAd aggregates. Formation of the pAd–MBP22 complex as calculated from the sedimentation profiles became satur-ated at high pAd concentrations (Figure 8B). Similar results were obtained for Tom20f and GST23 (Figure 8B). The pAd concentrations giving half-maximal complex formation indicated that the apparent affinities of the receptor domains for pAd increased in the order Tom20f<Tom22 (intermembrane)<Tim23 (intermem-brane) (Table I).

Sequential transfer of precursor from Tom70f via Tom20f and the internal Tom22 domain to Tim23

We have already shown that a precursor bound to MSF first docks onto the Tom70–Tom37 complex, is then transferred to the Tom20–Tom22 complex upon addition of ATP, and is finally transported into the mitochondria (Hachiya *et al.*, 1995). We tested whether this reaction sequence can be reproduced in the soluble system used here.

We incubated [^{125}I]pAd with unlabeled hsp70 and unlabeled MSF, and then added [^{125}I]Tom70f to form the pAd–MSF–Tom70f complex (Komiya *et al.*, 1996, 1997). This complex was incubated sequentially with [^{125}I]Tom20f in the presence or absence of ATP, with

A

B

Fig. 8. Determination of apparent pAd affinities of Tom20f, MBP22 and GST23. (**A**) The indicated concentrations of [^{125}I]pAd were incubated sequentially at 30°C for 15 min each with unlabeled hsp70 and with 7.5 nM [^{125}I]MBP22, and the mixtures were then analyzed by 5–20% sucrose density gradient centrifugation, SDS–PAGE and autoradiography. (**B**) Effect of pAd concentration on the formation of Tom20f–pAd, MBP22–pAd and GST23–pAd complexes. The amount of pAd in the receptor–pAd complexes (underlined) in (A) was quantified with a phosphorimager against a calibrated amount of [^{125}I]pAd. The pAd affinities of Tom20f and GST23 were measured at a fixed concentration of 7.5 nM Tom20f and 12.5 nM GST23 (sedimentation profiles not shown). Other conditions were the same as in (A), except that a 0–10% sucrose gradient was used for the experiment with Tom20f.

[^{125}I]MBP22, and with [^{125}I]GST23. Finally, the mixtures were analyzed by gradient centrifugation (Figure 9A). In the absence of ATP (Figure 9A, –ATP), pAd remained sequestered as the pAd–Tom70f–MSF complex (although the presence of MSF in the complex was not verified in this experiment, its presence has been documented before;
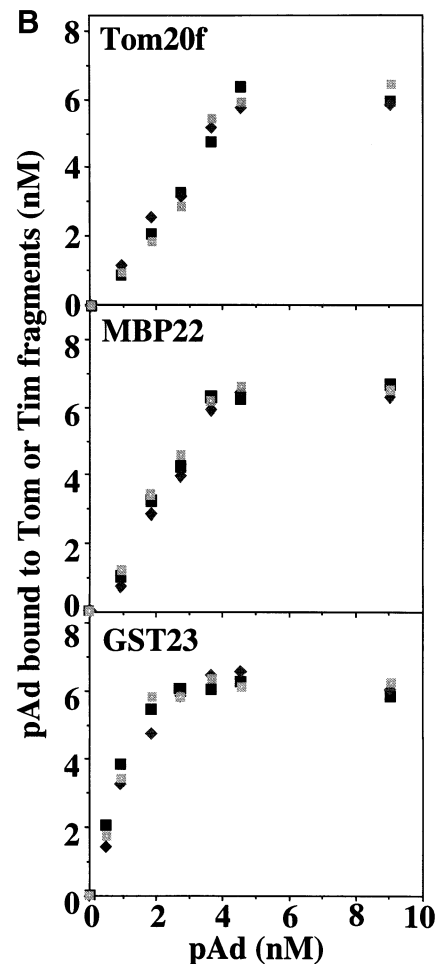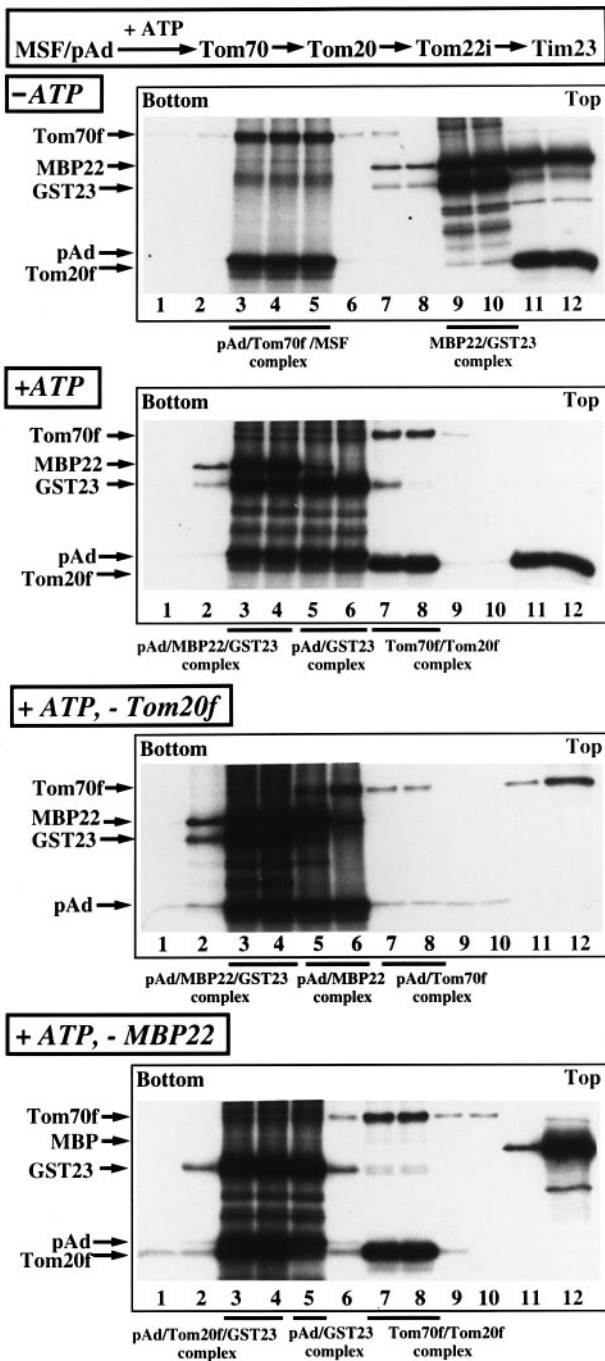
Komiya *et al*., 1997). Free MBP22 and Tom20f were detected in fractions 11 and 12, but part of MBP22 and all of GST23 sedimented as a complex with each other (fractions 9 and 10, immunoprecipitation data not shown). In the presence of ATP, the pAd–Tom70f–MSF complex dissociated and pAd was recovered as the pAd–GST23

Fig. 9. Transfer of pAd from Tom70f via Tom20f and MBP22 to GST23. (**A**) [^{125}I]pAd was incubated with unlabeled hsp70 and unlabeled MSF at 30°C for 15 min and then with [^{125}I]Tom70f for another 15 min in 100 μl of T20K50M1 buffer to form the pAd–MSF–Tom70f complex. This complex was incubated sequentially at 30°C for 15 min each with [^{125}I]Tom20f in the absence (–ATP) or the presence (+ATP) of 1 mM ATP, with [^{125}I]MBP22 and with [^{125}I]GST23. Finally, the mixtures were analyzed by gradient centrifugation, SDS–PAGE and autoradiography. Although not visible in this figure, repeats of the (+ATP) experiment sometimes revealed a small amount of GST23 in fractions 7 and 8. As controls, incubation with [^{125}I]Tom20f was omitted (+ATP, –Tom20f), or [^{125}I]MBP22 was replaced by [^{125}I]MBP (+ATP, –MBP22). (**B**) [^{125}I]pAd pre-bound to unlabeled hsp70 was incubated sequentially in 100 μl of T20K50M1 buffer at 30°C for 15 min each with [^{125}I]Tom20f, with [^{125}I]MBP22 (+MBP22) or [^{125}I]MBP (+MBP), and with [^{125}I]GST23. Finally, the mixtures were analyzed as in (A).

complex as well as the putative transfer intermediate (the pAd–MBP22–GST23 complex) (Figure 9A, +ATP). This result shows ATP-dependent transfer of pAd from MSF via Tom70f to the Tim23 domain. Omission of either Tom20f or the internal Tom22 domain from the transfer chain reaction significantly reduced formation of the pAd–GST23 complex (Figure 9A, –Tom20f and –MBP22; see also Table II). These results suggest that pAd is transferred sequentially and that Tom20f and the internal Tom22 domain increase the efficiency of the overall transfer reaction (Table II).

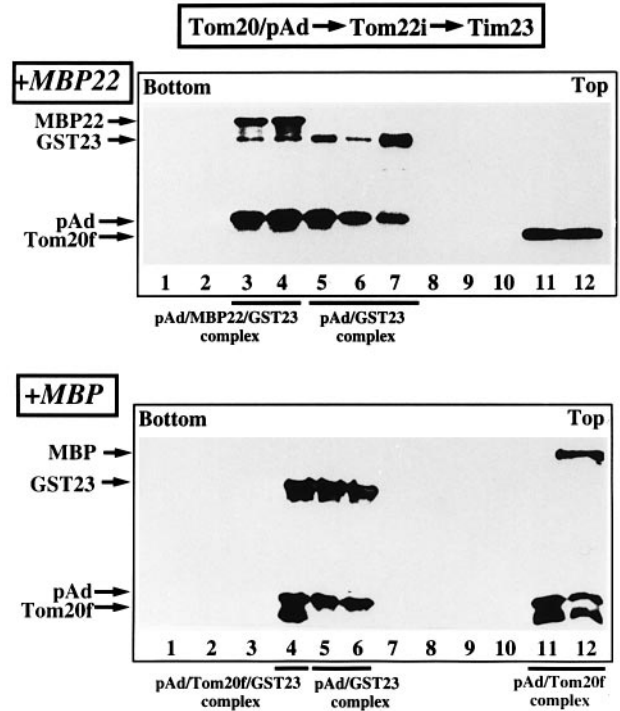To define the roles of Tom20f and the internal Tom22 domain more clearly, we generated the [^{125}I]pAd–[^{125}I]Tom20f complex as described in a previous section, incubated this complex sequentially with [^{125}I]MBP22 and [^{125}I]GST23, and analyzed the mixture by gradient centrifugation. As shown in Figure 9B (+MBP22), the entire pAd was released from Tom20f and recovered as a pAd–GST23 or pAd–MBP22–GST23 complex. The released Tom20f was detected in the top of the gradient. When [^{125}I]MBP22 was replaced by [^{125}I]MBP, transfer of pAd from Tom20f to GST23 was much less efficient: a significant fraction of the pAd–Tom20f complex remained intact and was recovered in the top fractions (Figure 9B, +MBP). Again, these results suggest that MBP22 increases the efficiency of the overall transfer reaction in

Table II. Distribution of the pAd–import receptor complexes in the reconstituted membrane-free transfer chains

System	Tom70f	→	Tom20f	→	Tom22i	→	Tim23i
Complete		70f–20f	20f			pAd–22i–23i (41%)	pAd–23i (54%)
Minus Tom20f	70f	pAd–70f–(22i)[a] (23%)			pAd–22i (22%)	pAd–22i–23i (47%)	
Minus Tom22i		70f–20f	pAd–20f–23i (58%)			pAd–23i	(31%)

System			Tom20f	→	Tom22i	→	Tim23i
Complete			20f			pAd–22i–23i (41%)	pAd–23i (50%)
Minus Tom22i			pAd–20f (32%)	pAd–20f–23i (21%)			pAd–23i (38%)

[a]A small amount of Tom22i was detected in the complex.
Relative amounts of pAd in the complexes were calculated from the fluoroimages taking the amount of input pAd as 100%.

Table III. Binding specificity of the import components for precursors targeted to different intramitochondrial compartments

Precursor	Final location	Tom70f	Tom20f	MBP22	GST23
Mdm12p	OM	ND	+	–	–
Porin	OM	+	+	–	–
CCHL	IMS	ND	+	+	–
AAC	IM	+	+	+	–
pAd	matrix	+	+	+	+
cpn10	matrix	ND	+	+	+

ND, not determined.
Binding is indicated by a + sign, lack of binding by a – sign.

the reconstituted system, perhaps because direct transfer from Tom20f to GST23 is kinetically disfavored (Table II).

To summarize, we can reconstitute sequential binding of a purified precursor to different purified receptor domains and show that transfer of the precursor between domains occurs more readily in the direction of the import pathway than in the reverse reaction.

Discussion

The 'acid chain' hypothesis
The aim of this study was to learn how precursor proteins are transported from the cytosol across the outer membrane into the intermembrane space. Although the outer membrane contains a protein transport channel (the TOM channel), it lacks a transmembrane electric potential and an ATP-dependent machinery which might be used to energize unidirectional transport of proteins across that channel.

A possible answer to this question was suggested by the observation that several components of the mitochondrial protein import system contain acidic domains which can bind the basic mitochondrial targeting signals (Bolliger *et al*., 1995; Bauer *et al*., 1996; Brix *et al*., 1997; Dietmeier *et al*., 1997; Komiya *et al*., 1997; Moczko *et al*., 1997; Rapaport *et al*., 1997; Schleiff *et al*., 1997). Such domains have been identified on both sides of the mitochondrial outer membrane as well as on the outer face of the inner membrane. Successive binding of a precursor's basic targeting signal to properly positioned acidic receptors of increasing affinity might thus effect net transfer of a
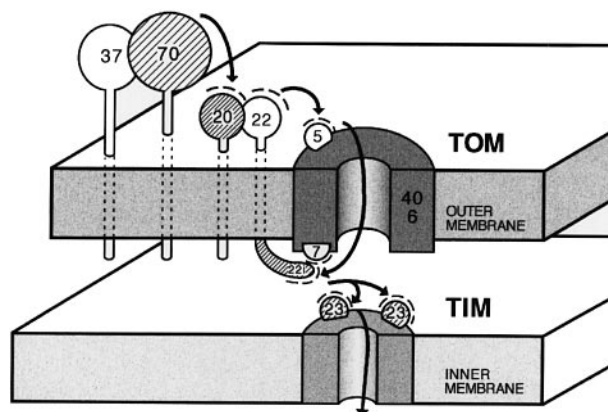

Fig. 10. The 'acid chain' hypothesis for protein transport across the mitochondrial outer membrane. See text for details. Acidic receptor domains are surrounded by minus signs. Proteins and protein domains examined in this study are shaded. Numbers designate the corresponding Tom and Tim proteins, and 22i the intermembrane space domain of Tom22. Arrows depict the pathway of a precursor into the matrix space.

precursor from the cytosol to the mitochondrial inner membrane. The last member of such an 'acid chain' would be cleared of bound precursor and reset for another round of binding by the combined action of the electric potential and the ATP-driven import motor of the inner membrane (Figure 10).

The assay
In order to test this hypothesis, we have used recombinant DNA methods to produce four soluble receptor domains

of the mitochondrial protein import system and have studied the interaction of these domains with mitochondrial precursor proteins and a mitochondrial targeting peptide. Two of the precursors were pure proteins, as were the cytosolic chaperones (hsp70 and MSF) that were used to present the precursors to the various receptor domains. Interaction of precursors with receptors was assayed by co-immunoprecipitation or by sucrose density gradient centrifugation.

How legitimate are such binding assays? While protein–protein interactions in a defined and water-soluble system offer obvious experimental advantages, they might be physiologically irrelevant. Also, our assays did not include all of the precursor-binding domains that have been identified along the mitochondrial protein import pathway. In order to resolve these uncertainties, it will be necessary to reconstitute a functional precursor-binding array with the correct transmembrane topology into liposomes, using the authentic receptor proteins. However, many of the interactions observed in the system described here are sufficiently specific to suggest that they indeed reflect the corresponding interactions *in vivo*. For example, binding of pAd to the different receptor domains is not observed with mature Ad (Komiya *et al.*, 1997 for Tom70f and Tom20f; data not shown for MBP22 and GST23); binding is inhibited by a mitochondrial targeting peptide, but not by a control peptide; binding to Tom20f and the internal Tom22 domain is sensitive to 150 mM NaCl, as it is in mitochondria; and binding to the acidic receptor domains increases in the order in which these domains act in the import pathway.

It is also striking that the three acidic receptor domains examined here exhibit a strict recognition specificity for precursor proteins destined for distinct intramitochondrial compartments (Table III). Tom20f recognizes all of the precursor proteins examined; MBP22 recognizes precursors destined for the inside of the outer membrane; and GST23 recognizes only matrix-targeted precursors. It will be intriguing to learn whether the precursor-binding specificity of the cytosolic Tom22 domain exhibits the same specificity as that of Tom20. If so, the result would strengthen further the suggestion that the precursor specificity of receptors located inside the mitochondria may help to sort imported proteins to specific intramitochondrial compartments.

The finding that GST23 does not recognize the AAC precursor is consistent with the observation that import of this protein is mediated mainly by the Tim10–Tim12–Tim22 complex whereas import of matrix-targeted precursors is mediated by the Tim23–Tim17 complex (Sirrenberg *et al.*, 1996; Koehler *et al.*, 1998). On the other hand, antibodies against Tim23 inhibit the insertion of AAC into inner membrane vesicles, and a detergent extract of mitochondria immunodepleted of Tim23 can no longer be reconstituted into vesicles inserting radiolabeled AAC (Haucke and Schatz, 1997). A possible role for Tim23 in AAC import thus deserves further study.

We are intrigued by the fact that Tom20f and the internal Tom22 domain enhance precursor transfer from Tom70f to Tim23, and from Tom20 to Tim23, respectively. A similar 'coupling' effect might function in other steps in the postulated 'acid chain'. By minimizing illegitimate bypass reactions, such coupling may contribute to the fidelity of intramitochondrial protein sorting.

The structural basis for these specific interactions remains unknown. Inspection of the primary sequences of the charged receptor domains has not revealed any special features that could explain the specific recognitions observed here.

The detection of a MBP22–GST23 complex in the absence of pAd transfer (Figure 8A, –ATP, fractions 9 and 10) is intriguing. This complex was resistant to 150 mM potassium acetate (data not shown). Its existence suggests the possibility that transient docking of the TOM and TIM complexes during protein import into the matrix (Horst *et al.*, 1995) may be mediated partly by interaction between the intermembrane space domains of Tom22 and Tim23.

The function of the internal Tom22 domain in protein import has been controversial. While Bolliger *et al.* (1995) reported that this domain specifically binds basic mitochondrial targeting signals and contributes to the import process, both Nakai *et al.* (1995) and Court *et al.* (1996a) failed to detect such functions. Recently, Moczko *et al.* (1997) confirmed that this domain accelerates protein import by functioning as a *trans* binding site for insertion of the precursors across the Tom channel (Moczko *et al.*, 1997). However, Moczko *et al.* also showed that this domain did not influence the import of the AAC precursor into intact mitochondria, whereas we find that this domain binds the AAC precursor. This discrepancy remains unexplained. Binding to this domain might not be rate limiting for AAC import *in vivo*. Alternatively, deletion of the internal Tom22 domain from some yeast strains might cause up-regulation of other precursor-binding sites (Mayer *et al.*, 1995a) on the inner face of the outer membrane. An example of a compensatory interaction between mitochondrial import receptors has been reported by Lithgow *et al.* (1994).

Specific interaction of mitochondrial precursors with the cytosolic domain of human (Schleiff *et al.*, 1997) or yeast (Brix *et al.*, 1997) Tom20 was also observed by others. In agreement with our results, Brix *et al.* detected specific inhibition of binding by a mitochondrial targeting peptide. In contrast to our findings, however, the binding observed by them was enhanced by salt.

To summarize, our results are compatible with the 'acid chain' hypothesis according to which transfer of precursors across the mitochondrial outer membrane is mediated by increasingly tight binding of the precursor's targeting signal to acidic binding sites on both sides of the outer membrane.

Materials and methods

Expression and purification of MBP22 and GST23

The intermembrane space domain of Tom22p (A121–N154) was amplified with *Pfu* polymerase (Stratagene Corp.) by PCR and inserted as an *Sst*I–*Hin*dIII fragment into the multiple cloning region of pMAL-c2 (New England Biolabs) so that the C-terminal tail of Tom22p was fused to the C-terminus of *E.coli* MBP. The intermembrane space domain of Tim23p (M1–D96) was amplified with *Pfu* polymerase by PCR and inserted as a *Sma*I–*Xho*I fragment into the multiple cloning region of pGEX-4T-1 (Pharmacia Biotech) so that the N-terminus of Tim23p was fused to the C-terminus of *S.japonicum* GST. These fusion proteins were overexpressed in *E.coli* strain DH10b. Fusion protein MBP22 was purified according to Bolliger *et al.* (1995). Fusion protein GST23 was

purified by the same method as MBP22 except that glutathione–Sepharose beads (Sigma Corp.) were used to recover the fusion protein from the *E.coli* lysate. After elution from the affinity beads, the eluate buffer containing the fusion protein was exchanged for 20 mM Tris–HCl, pH 8.0 in a Centricon 30 microconcentrator (Amicon Corp.) and frozen at –80°C at a protein concentration of 3–5 mg/ml. This method yielded 20–40 mg of MBP22 and 2–5 mg of GST23 protein per liter of *E.coli* culture, respectively.

Interaction of precursor proteins with MBP22 or GST23

Binding of precursor proteins to MBP22 was tested by incubating 0.5 pmol of ^{125}I-labeled recombinant precursors (pAd, porin or cpn10) in a final volume of 50 µl for 20 min at 30°C with 2.5 pmol of [125I]hsp70 in 20 mM Tris–HCl pH 7.5, 100 mM potassium acetate, 2 mM magnesium acetate (T20K100M2 buffer). The reaction mixtures were diluted 2-fold with 20 mM Tris–HCl pH 7.5 (to yield T20K50M1) and incubated with 7.5 pmol of either [125I]MBP22 or [125I]MBP at 30°C for 20 min (final concentrations in µM: pAd or porin, 0.005; hsp70, 0.025; MBP22 or MBP, 0.0075; GST23 or GST, 0.0125). Finally, the mixtures were subjected to immunoprecipitation with IgGs against Ad or MBP as described (Komiya *et al*., 1996), except that immunoprecipitates were washed with 20 mM phosphate buffer pH 7.0 containing 0.05% Tween-20. Where indicated, the synthetic mitochondrial targeting peptide SCC1-19 or the non-functional control peptide SynB2 was added together with [125I]MBP22. For assaying binding of CCHL, Mdm12p or AAC (Komiya *et al*., 1997), 10 µl of ^{35}S-labeled precursor proteins which had been synthesized in a wheat germ lysate and dialyzed overnight against 10 mM HEPES–KOH pH 7.4, 7 M urea, 1 mM EDTA, 1 mM phenylmethylsulfonyl fluoride (PMSF) were incubated in 500 µl of T20K50M1 with [125I]hsp70, [125I]MBP22 or [125I]MBP as described above, followed by immunoprecipitation with IgGs against MBP. Binding of precursor proteins to GST23 was performed as for MBP22, except that 0.0125 µM [125I]GST23 or [125I]GST were used instead of MBP22. Reaction mixtures were then incubated with glutathione–Sepharose beads, the beads were washed with 20 mM sodium phosphate buffer pH 7.0, 0.05% Tween-20, and adsorbed proteins were eluted by SDS-containing sample buffer and analyzed by SDS–PAGE and autoradiography. Interaction of the precursor with Tom20f was assayed as described (Komiya *et al*., 1997), except that the immunoprecipitates were washed with 20 mM sodium phosphate buffer pH 7.0, 0.05% Tween-20.

Transfer of pAd from the pAd–MSF–Tom70f to Tom70f

[125I]pAd was incubated with unlabeled hsp70 and unlabeled MSF in 50 µl of T20K100M2 at 30°C for 20 min. The reaction mixture was then incubated at 30°C for 20 min each with [125I]Tom70f and 1 mM ATP in 100 µl of T20K50M1.

Transfer of AAC from Tom20f to MBP22 or from MBP22 to Tom20f

Transfer of AAC from Tom20f to MBP22 was performed as follows. A 10 µl aliquot of ^{35}S-labeled AAC that had been synthesized in a wheat germ lysate was dialyzed against 10 mM HEPES–KOH (pH 7.4), 7 M urea, 1 mM EDTA, 1 mM PMSF and sequentially incubated in 500 µl of T20K50M1 at 30°C for 20 min each with [125I]hsp70, with [125I]Tom20f and with either [125I]MBP or [125I]MBP22. Finally, the mixture was analyzed by gradient centrifugation and SDS–PAGE as described (Komiya *et al*., 1997) except that 0.46 ml fractions were collected from the top of each tube. The final concentrations of hsp70, Tom20f and MBP22 in the incubation mixture were 0.025, 0.0075 and 0.0075 µM, respectively. Where indicated, a 3-fold molar excess of unlabeled MBP22 was included [Figure 2A, +MBP22 (×3)]. To assay for reverse transfer of AAC from MBP22 to Tom20f, a 10 µl aliquot of [35S]AAC was bound to [125I]hsp70 as described above, incubated sequentially at 30°C for 20 min each with [125I]MBP22 and [125I]Tom20f, and analyzed by gradient centrifugation and SDS–PAGE. Where indicated, a 3-fold molar excess of unlabeled Tom20f was included [Figure 3, +20f (×3)].

Transfer of pAd from MBP22 to GST23 or from GST23 to MBP22

For transfer of pAd from MBP22 to GST23, [125I]pAd was incubated with unlabeled hsp70 in 50 µl of T20K100M2 at 30°C for 20 min, then incubated sequentially in 100 µl of T20K50M1 at 30°C for 20 min each with [125I]MBP22 and either [125I]GST or [125I]GST23, and analyzed by gradient centrifugation and SDS–PAGE. The final concentrations of pAd, hsp70, MBP22 and GST23 were 0.005, 0.025, 0.0075 and

0.0125 µM, respectively. Where indicated, a 1- or 3-fold molar excess of unlabeled GST23 was added [Figure 6A, +GST23 (×1), +GST23 (×3)].

For reverse transfer of pAd from GST23 to MBP22, [125I]pAd was incubated with unlabeled hsp70 in 50 µl of T20K100M2 at 30°C for 20 min, incubated sequentially in 100 µl of T20K50M1 at 30°C for 20 min each with GST23 and MBP22 and then analyzed by gradient centrifugation and SDS–PAGE. The final concentrations of pAd, hsp70, GST23 and MBP22 were 0.005, 0.025, 0.0125 and 0.0075 µM, respectively. Where indicated, a 3-fold molar excess of unlabeled MBP22 was added [Figure 6C, +MBP22 (×3)].

ATP-dependent transfer of pAd from the pAd–MSF–Tom70f complex via Tom20f and MBP22 to GST23

[125I]pAd pre-incubated with unlabeled hsp70 and unlabeled MSF in 50 µl of T20K100M2 buffer at 30°C for 15 min was incubated sequentially in 100 µl of T20K50M1 buffer at 30°C for 15 min each with [125I]Tom70f, [125I]Tom70f plus 1 mM ATP, [125I]MBP22 and [125I]GST23. As controls, we either omitted Tom20f or replaced [125I]MBP22 by [125I]MBP (Figure 9A). Finally, the mixture was analyzed by gradient centrifugation and SDS–PAGE. The final concentrations of pAd, hsp70, MSF, Tom70f, Tom20f, MBP22 and GST23 were 0.005, 0.025, 0.007, 0.0075, 0.0075, 0.0075 and 0.0125 µM, respectively.

Transfer of pAd from Tom20f via MBP22 to GST23

[125I]pAd pre-incubated with unlabeled hsp70 in 50 µl of T20K100M2 buffer at 30°C for 15 min was incubated sequentially in 100 µl of T20K50M1 buffer at 30°C for 15 min each with [125I]Tom20f, [125I]MBP22 and [125I]GST23. Finally, the mixture was analyzed by gradient centrifugation and SDS–PAGE. The final concentrations of pAd, hsp70, Tom20f, MBP22 and GST23 were 0.005, 0.025, 0.0075, 0.0075 and 0.0125 µM, respectively. As a control, [125I]MBP was added instead of [125I]MBP22.

Determination of K_d values of the import receptors for pAd

Binding of pAd to Tom20f, MBP22 or GST23 was measured at the indicated pAd concentrations as described above (Figure 8B; final concentrations, 0, 0.9, 1.8, 2.7, 3.6, 4.5 and 9 nM). In addition to these concentrations, binding to GST23 was also measured with 0.45 nM pAd. Each experimental point was measured in three independent experiments. The receptor–pAd complexes were analyzed by 0–10% sucrose (for Tom20f) or 5–20% sucrose (for MBP22 and GST23) density gradient centrifugations. Other conditions are as described (Komiya *et al*., 1997). The amount of pAd in each complex was calculated from the phosphorimages using samples of [125I]pAd as the standard.

Determination of the concentration of [125I]pAd

[125I]pAd and unlabeled pAd (0.1–2.5 µg) were subjected to SDS–PAGE and the gels were stained by 'SYPRO Orange protein gel stain' according to the manufacturer's protocol (Molecular Probes, Inc.). Fluoroimages of the stained gels were analyzed by FLA2000 (Fuji Film) and the protein concentration of [125I]pAd was calculated using unlabeled pAd as the standard.

Isolation of the yeast genes for cytochrome c heme lyase (CCHL) and Mdm12p

Yeast genes for CCHL (*CYC3*; Dumont *et al*., 1987) and Mdm12p (*MDM12*; Berger *et al*., 1997) were isolated by PCR using yeast genomic DNA as the template and the following oligonucleotides as the primers: sense strand for CCHL, 5′-TCAGAGTAGCAC*GAATTC*AGCAGA-3′; antisense strand for CCHL, 5′-ATAAAGGTG*AAGCTT*GTGATAATA-3′; sense strand for Mdm12p, 5′-GCT*GAATTC*AACTAATCCAAATGT-CTTTTG-3′; antisense strand for Mdm12p, 5′-GTT*AAGCTT*GG-ATTACTTCCTGACAAAAT-3′, where underlining indicates *Eco*RI and *Hin*dIII sites, respectively.

Both PCR fragments were cloned into *Eco*RI–*Hin*dIII-digested vector pSP65 and used for *in vitro* transcription.

Miscellaneous

MSF was purified from rat liver cytosol (Hachiya *et al*., 1993). pAd and porin were expressed in *E.coli* and purified in 7 M urea (Iwahashi *et al*., 1992). The cytosolic domains of the yeast mitochondrial receptor subunits Tom20 and Tom70 were expressed in *E.coli* and purified as described (Komiya *et al*., 1997). Yeast mitochondrial cpn10 was expressed in *E.coli* and purified as described (Dubaquié *et al*., 1997). Monospecific IgGs against Ad, yeast Tom20 and *E.coli* MBP are either as described (Ramage *et al*., 1993; Komiya *et al*., 1997) or were obtained commercially. Precursor proteins for AAC, CCHL and Mdm12p were synthesized

in a wheat germ lysate in the presence of [^{35}S]methionine and dialyzed overnight against 10 mM HEPES–KOH (pH 7.4), 1 mM EDTA, 1 mM PMSF, 7 M urea. pAd, porin, cpn10, hsp70, Tom70f, Tom20f, MBP22, MBP, GST23 and GST were ^{125}I-labeled (Komiya *et al.*, 1996) using Iodo-Beads (Pierce Co.) to a final specific radioactivity of 0.6–1.0×10^8 c.p.m./mg protein. Protein concentrations were assayed by the Protein Assay system sold by Bio-Rad Co., using bovine serum albumin as the standard. Molar concentrations of proteins were calculated assuming the following molecular masses (in kDa): pAd, 22; porin, 29; hsp70, 70; MSF, 58; Tom20f, 20; Tom70f, 70; MBP22, 47; MBP, 48; GST23, 40; and GST, 30.

Acknowledgements

References

Bauer,M.F., Sirrenberg,C., Neupert,W. and Brunner,M. (1996) Role of Tim23 as voltage sensor and presequence receptor in protein import into mitochondria. *Cell*, **87**, 33–41.

Berger,K.H., Sogo,L.F. and Yaffe,M.P. (1997) Mdm12p, a component required for mitochondrial inheritance that is conserved between budding and fission yeast. *J. Cell Biol.*, **136**, 545–553.

Bolliger,L., Junne,T., Schatz,G. and Lithgow,T. (1995) Acidic receptor domains on both sides of the outer membrane mediate translocation of precursor proteins into yeast mitochondria. *EMBO J.*, **14**, 6318–6326.

Brix,J., Dietmeier,K. and Pfanner,N. (1997) Differential recognition of preproteins by the purified cytosolic domains of the mitochondrial import receptors Tom20, Tom22 and Tom70. *J. Biol. Chem.*, **272**, 20730–20735.

Court,D.A., Nargang,F.E., Steiner,H., Hodges,R.S., Neupert,W. and Lill,R. (1996a) Role of the intermembrane-space domain of the preprotein receptor Tom22 in protein import into mitochondria. *Mol. Cell Biol.*, **16**, 4035–4042.

Court,D.A., Kleene,R., Neupert,W. and Lill,R. (1996b) Role of the N-and C-termini of porin in import into the outer membrane of *Neurospora* mitochondria. *FEBS Lett.*, **390**, 73–77.

Dietmeier,K., Honlinger,A., Bomer,U., Dekker,P.J.T., Eckerskorn,C., Lottespeich,F., Kubrich,M. and Pfanner,N. (1997) Tom5 functionally links mitochondrial preprotein receptors to the general insertion pore. *Nature*, **388**, 195–200.

Dubaquié,Y., Looser,R. and Rospert,S. (1997) Significance of chaperonin 10-mediated inhibition of ATP hydrolysis by chaperonin 60. *Proc. Natl Acad. Sci. USA*, **94**, 9011–9016.

Dumont,M.E., Ernst,J.F., Hampsy,D.M. and Sherman,F. (1987) Identification and sequence of the gene encoding cytochrome *c* heme lyase in the yeast *Saccharomyces cerevisiae*. *EMBO J.*, **6**, 235–241.

Hachiya,N., Alam,R., Sakasegawa,Y., Sakaguchi,M., Mihara,K. and Omura,T. (1993) A mitochondrial import factor purified from rat liver cytosol is an ATP-dependent conformational modulator for precursor proteins. *EMBO J.*, **12**, 1579–1586.

Hachiya,N., Mihara,K., Suda,K., Horst,M., Schatz,G. and Lithgow,T. (1995) Reconstitution of the initial steps of mitochondrial protein import. *Nature*, **376**, 705–709.

Haucke,V. and Schatz,G. (1997) Reconstitution of the protein insertion machinery of the mitochondrial inner membrane. *EMBO J.*, **16**, 4560–4567.

Haucke,V., Lithgow,T., Rospert,S., Hahne,K. and Schatz,G. (1995) The yeast mitochondrial protein import receptor Mas20p binds precursor proteins through electrostatic interaction with the positively charged presequence. *J. Biol. Chem.*, **270**, 5566–5570.

Hönlinger,A. *et al.* (1995) The mitochondrial receptor complex: Mom22 is essential for cell viability and directly interacts with preproteins. *Mol. Cell. Biol.*, **15**, 3382–3389.

Horst,M., Oppliger,W., Rospert,S., Schönfeld,H.-J., Schatz,G. and Azem,A. (1995) Dynamic interaction of the protein translocation systems in the inner and outer membranes of yeast mitochondria. *EMBO J.*, **14**, 2293–2297.

Iwahashi,J., Furuya,S., Mihara,K. and Omura,T. (1992) Characterization of adrenodoxin precursor expressed in *Escherichia coli*. *J. Biochem.*, **111**, 451–455.

Koehler,C.M., Jarosch,E., Tokatlidis,K., Schmid,K., Schweyen,R.J. and Schatz,G. (1998) Import of mitochondrial carriers mediated by essential proteins of the intermembrane space. *Science*, **279**, 369–373.

Komiya,T., Sakaguchi,M. and Mihara,M. (1996) Cytoplasmic chaperones determine the targeting pathway of precursor proteins to mitochondria. *EMBO J.*, **15**, 399–407.

Komiya,T., Rospert,S., Schatz,G. and Mihara,K. (1997) Binding of mitochondrial precursor proteins to the cytoplasmic domains of the import receptors Tom70 and Tom20 is determined by cytoplasmic chaperones. *EMBO J.*, **16**, 4267–4275.

Lill,R., Nargang,F.E. and Neupert,W. (1996) Biogenesis of mitochondrial proteins. *Curr. Opin. Cell Biol.*, **8**, 505–512.

Lithgow,T., Junne,T., Suda,K., Gratzer,S. and Schatz,G. (1994) The mitochondrial outer membrane protein Mas22p is essential for protein import and viability. *Proc. Natl Acad. Sci. USA*, **91**, 11973–11977.

Lithgow,T., Glick,B.S. and Schatz,G. (1995) The protein import receptor of mitochondria. *Trends Biochem. Sci.*, **20**, 98–101.

Mayer,A., Neupert,W. and Lill,R. (1995a) Mitochondrial protein import: reversible binding of the presequence at the *trans* side of the outer membrane drives partial translocation and unfolding. *Cell*, **80**, 127–137.

Mayer,A., Nargang,F.E., Nuepert,W. and Lill,R. (1995b) MOM22 is a receptor for mitochondrial targeting sequences and cooperates with MOM19. *EMBO J.*, **14**, 4204–4211.

Mihara,K. and Omura,T. (1996) Cytoplasmic chaperones in precursor targeting to mitochondria: the role of MSF and hsp70. *Trends Cell Biol.*, **6**, 104–108.

Moczko,M., Bömer,U., Küblich,M., Zufall,N., Hönlinger,A. and Pfanner,N. (1997) The intermembrane space domain of mitochondrial Tom22 functions as a *trans* binding site for preproteins with N-terminal targeting sequences. *Mol. Cell. Biol.*, **17**, 6574–6584.

Nakai,M., Kinoshita,K. and Endo,T. (1995) Mitochondrial receptor complex protein. The intermembrane space domain of yeast MAS17 is not essential for its targeting or function. *J. Biol. Chem.*, **270**, 30571–30575.

Neupert,W. (1997) Protein import into mitochondria. *Annu. Rev. Biochem.*, **66**, 863–917.

Pfanner,N., Hoeben,P., Tropschung,M. and Neupert,W. (1987) The carboxyl-terminal two-thirds of the ADP/ATP carrier polypeptide contains sufficient information to direct translocation into mitochondria. *J. Biol. Chem.*, **262**, 14851–14854.

Ramage,L., Junne,T., Hahne,K., Lithgow,T. and Schatz,G. (1993) Functional cooperation of mitochondrial protein import receptors in yeast. *EMBO J.*, **12**, 4115–4123.

Rapaport,D., Neupert,W. and Lill,R. (1997) Mitochondrial protein import. Tom40 plays a major role in targeting and translocation of preproteins by forming a specific binding site for the presequence. *J. Biol. Chem.*, **272**, 18725–18731.

Schatz,G. (1996) The protein import system of mitochondria. *J. Biol. Chem.*, **271**, 31763–31766.

Schatz,G. (1997) Just follow the acid domain. *Nature*, **388**, 121–122.

Schatz,G. and Dobberstein,B. (1996) Common principles of protein translocation across membranes. *Science*, **271**, 1519–1526.

Schleiff,E., Shore,G.C. and Goping,I.S. (1997) Interactions of the human mitochondrial protein import receptor, hTom20, with precursor proteins *in vitro* reveal pleiotropic specificities and different receptor domain requirements. *J. Biol. Chem.*, **272**, 17784–17789.

Sirrenberg,C., Bauer,M.,F., Guiard,B., Neupert,W. and Brunner,M. (1996) Import of carrier proteins into the mitochondrial inner membrane mediated by Tim22. *Nature*, **384**, 582–585.